Nuclear Data for Science and Technology (1988 MITO), 691- 694, Copyright © 1988 JAERI.

OPTICAL MODEL ANALYSIS OVER A WIDE RANGE OF NUCLEI USING POLARIZED NEUTRON SCATTERING DATA

G. Schreder, J.W. Hammer, W. Grum, K.-W. Hoffmann, G. Dagge, M. Koch, G. Bulski, G. Keilbach, H. Postner and G. Schleußner

Universität Stuttgart, Institut für Strahlenphysik
Allmandring 3, 7000 Stuttgart 80, Federal Republic of Germany

P.A. Owono

Departement de Physique, Université de Yaounde, Kamerun

Abstract: Polarized neutron scattering data for the nuclei ^{27}Al, ^{nat}Cr, ^{nat}Cu, ^{89}Y, ^{nat}W, ^{nat}Pb, ^{209}Bi, ^{232}Th and ^{238}U were analyzed in terms of spherical, coupled channels and microscopic optical model potentials. The measurements at typical 7.75 MeV neutron energy were performed at the Stuttgart SCORPION facility.

(Diff. cross section, Analyzing power, spherical, coupled channels, microscopic optical model)

Introduction

Analysing power data together with the corresponding differential cross section measurements not only provide a better determination of optical model spin-orbit parameters, but also reduce the ambiguities inherent in the other parts of phenomenological potentials. They thus constitute an important data base for testing whatever model potential.

At the Stuttgart SCORPION facility polarized neutron scattering on a large number of nuclei at an incident neutron energy of typical 7.75 MeV has been investigated during the past years. Most of the data have been analyzed in terms of the conventional spherical optical model as well as coupled–channels calculations in the case of collectively excited nuclei. The application of microscopic potentials from various nuclear matter approaches is in progress.

Experimental Method

Polarized neutrons were produced in the reaction ^{9}Be(α,n)^{12}C with the 500μA α-current of the 4 MeV Dynamitron. The $\vec{n}$–production target, a spin-flip magnet, 4 NE213-detectors and 4 monitors are located in a close doubly shielded geometry. The contribution of γ-events could be kept below typically 1% by means of sophisticated n-γ–discrimination circuits. The background-substracted pulse height spectra were unfolded with the code FANTI [1]. The calibration of the setup to absolute cross section values was performed by normalization to the hydrogen cross section using a polyethylene sample. Corrections due to flux attenuation, multiple scattering and depolarization in the scattering sample were carried out with the Monte Carlo code XJANE [2]. A more detailed description of the experimental setup and the various methods of data evaluation can be found in Ref. [1].

Phenomenological Optical Model Analysis

For both spherical and deformed nuclei the code ECIS79 [3] was employed, which uses a potential of the following form:

$$U(r) = -V_R f_V(r) + 4 i a_D W_D g_D(r) + \lambda_\pi^2 (V_{SO} + i W_{SO}) \frac{1}{r} g_{SO}(r) \left(2 \vec{\ell} \cdot \vec{s} \right), \quad (1)$$

with the Woods-Saxon form factors

$$f_X(r) = \frac{1}{1 + exp\left(\frac{r - R_X}{a_X}\right)}, \quad g_X(r) = \frac{df_X}{dr}, \quad (2)$$

where X = R, D, SO stands for real, imaginary surface derivative and spin-orbit terms, respectively. The nuclear radius R is given by $R = R_o = r_o A^{1/3}$ for spherical nuclei. In the case of deformed nuclei the radius is expressed by an expansion in Spherical Harmonics.

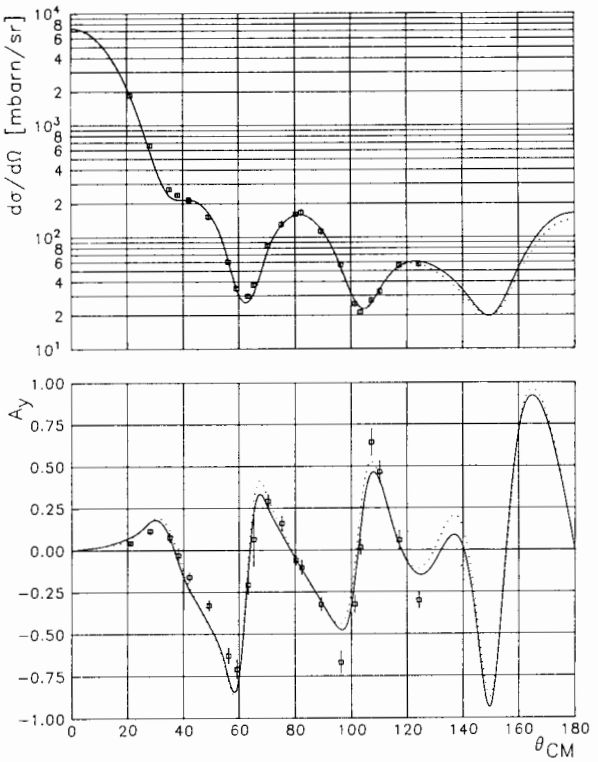

Fig. 1: Differential cross section and analysing power of ^{nat}Pb. SOM calculations were done with (full) and without (dotted) W_{so}.

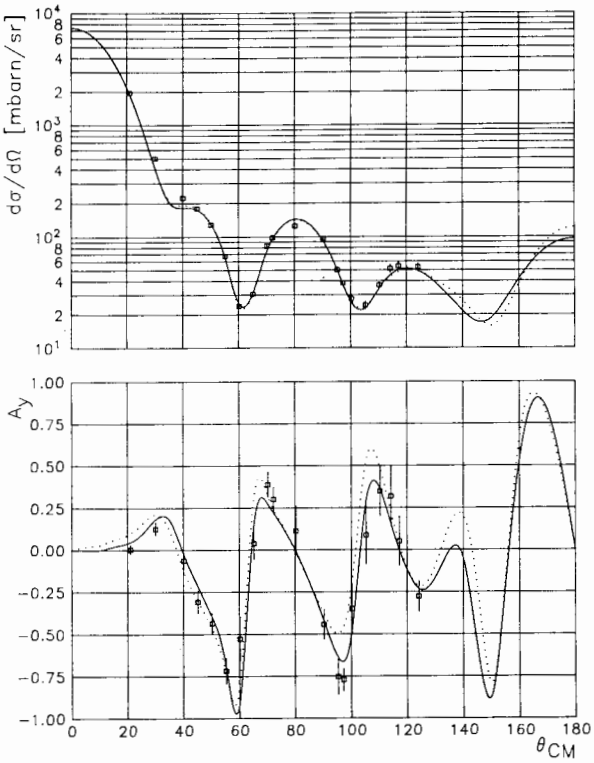

Fig. 2: Differential cross section and analysing power of ^{209}Bi. SOM calculations were done with (full) and without (dotted) W_{so}.

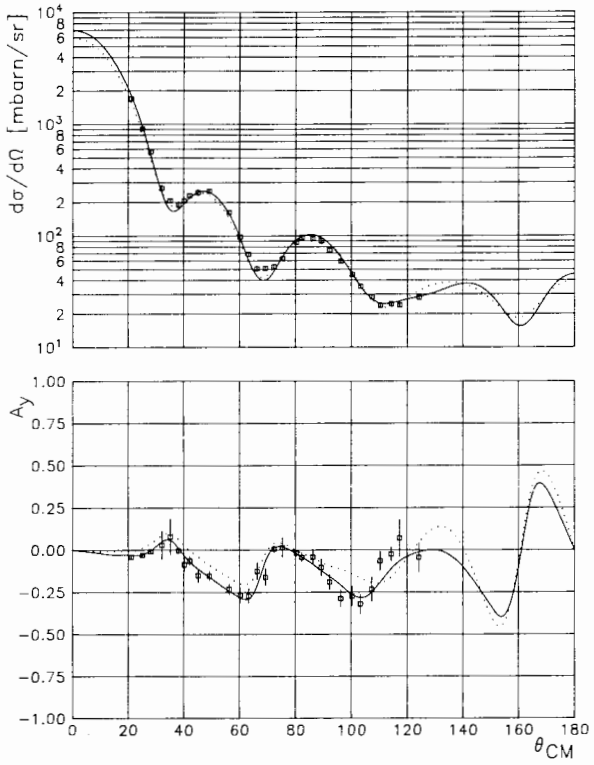

Fig. 3: Differential cross section and analysing power of ^{nat}W. CC calculations were done with (full) and without (dotted) W_{so}.

Spherical Model Analysis (SOM)

The results for ^{nat}**Pb** and ^{209}**Bi** are shown in Figs. 1 and 2. The calculations revealed much better results when the imaginary spin-orbit term was included in the above model potential (see for instance Ref. [4]).

Coupled Channels Analysis (CC)

In the analysis for the nuclei ^{nat}**W**, ^{232}**Th** and ^{238}**U** it again turned out that the inclusion of W_{so} lead to a significant improvement of the model fits. The results are shown in Figs. 3, 4 and 5.

^{27}**Al** was treated as a $2d_{5/2}$ proton hole weakly coupled to a ^{28}Si core. According to the model description of silicon a rotational coupling scheme $0^+ - 2^+$ with the deformation parameters of Si was used. The excited 2^+ – state is split into a quintet without changing the shape of the inelastic cross section. The above model, already successfully applied for the description of differential cross sections at 11, 14 and 17 MeV [5], is also supported by the analysing power data of this work (see Fig. 6). The large compound scattering contributions were calculated with the code CERBERO [6], but to get the correct CC–transmission coefficients, the corresponding input of ECIS79 was adjusted in 'SOM–mode' to get the same results.

^{nat}**Cr** is composed of 83% ^{52}Cr and 17% ^{53}Cr. Provided the excited core model holds also for ^{53}Cr, the scattering data should be similar for both isotopes. The calculations with the harmonic vibrational model agree quite well with the data, but as the level scheme of the ^{52}Cr – core indicates an anharmonic vibrator, the results given in Fig. 7 were also calculated with an anharmonic model.

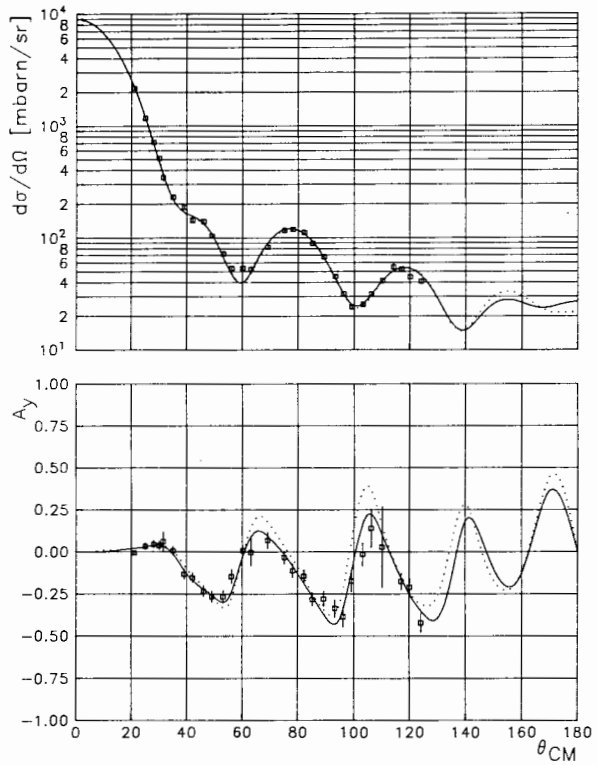

Fig. 4: Differential cross section and analysing power of ^{232}Th. CC calculations were done with (full) and without (dotted) W_{so}.

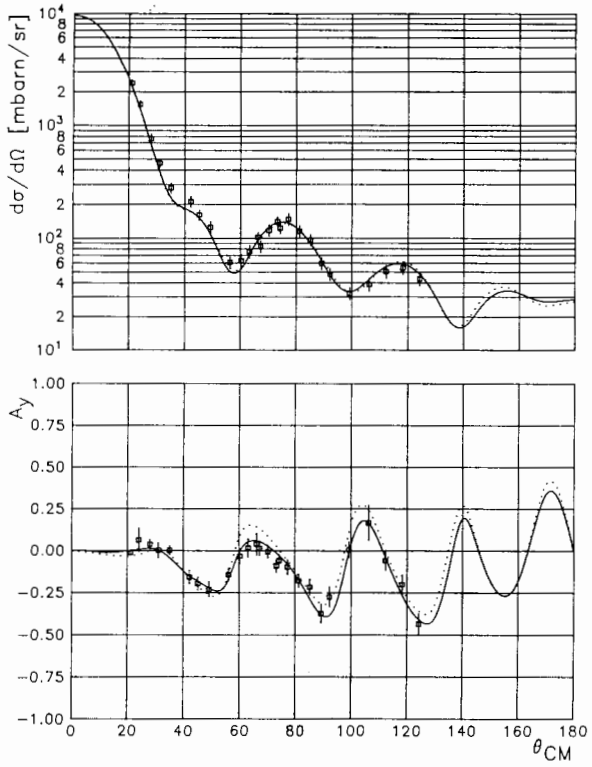

Fig. 5: Differential cross section and analysing power of ^{238}U. CC calculations were done with (full) and without (dotted) W_{so}.

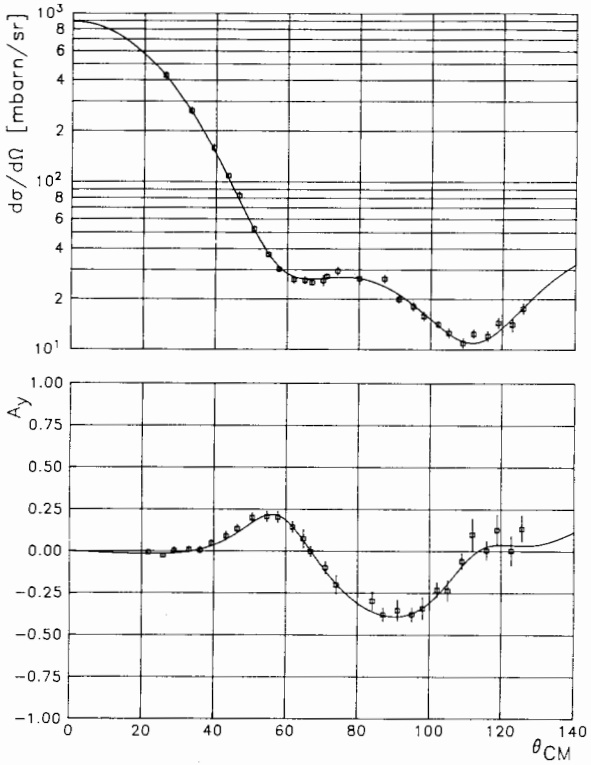

Fig. 6: Differential cross section and analysing power of ^{27}Al together with CC model results.

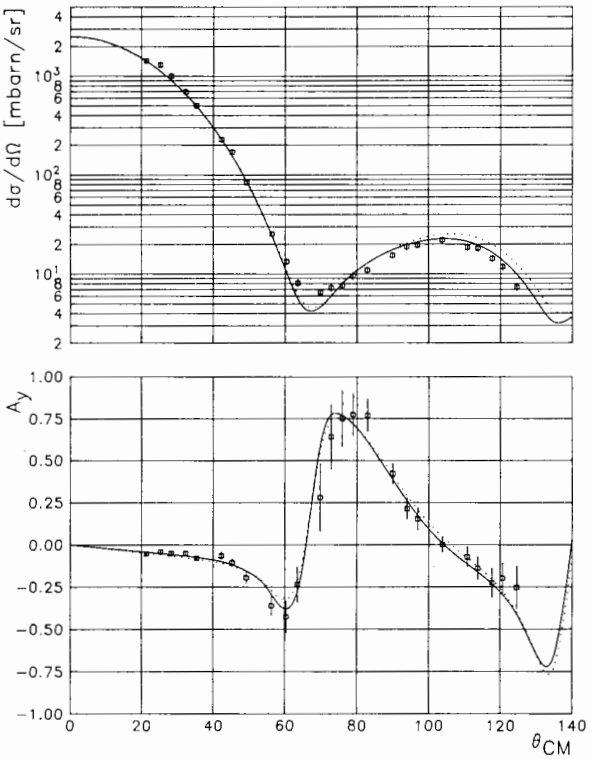

Fig. 7: Differential cross section and analysing power of ^{nat}Cr. CC calculations were done with an anharmonic (full) and a harmonic (dotted) vibrational model.

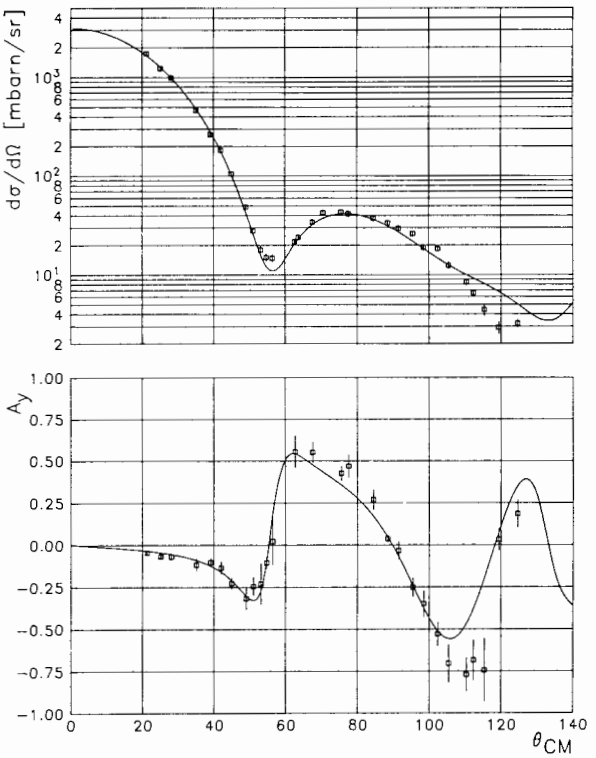

Fig. 8: Differential cross section and analysing power of ^{nat}Cu together with CC model results.

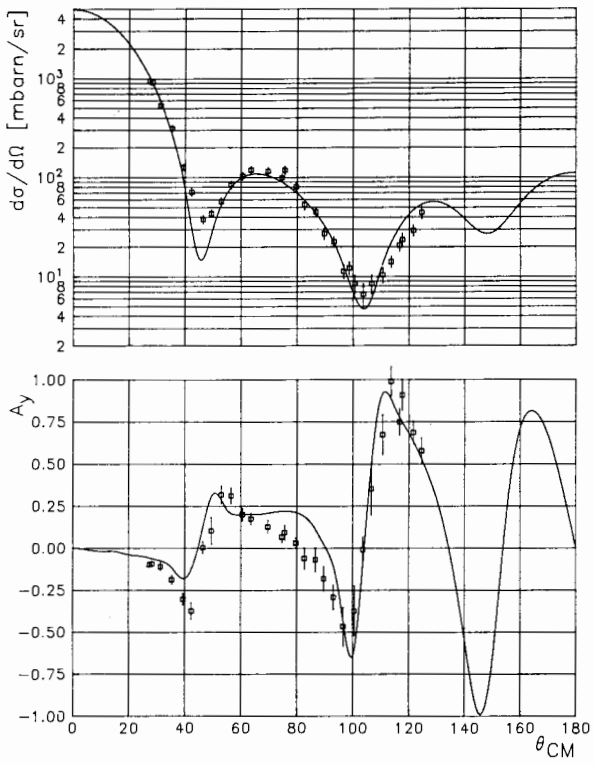

Fig. 9: Differential cross section and analysing power of ^{89}Y together with microscopic optical model results.

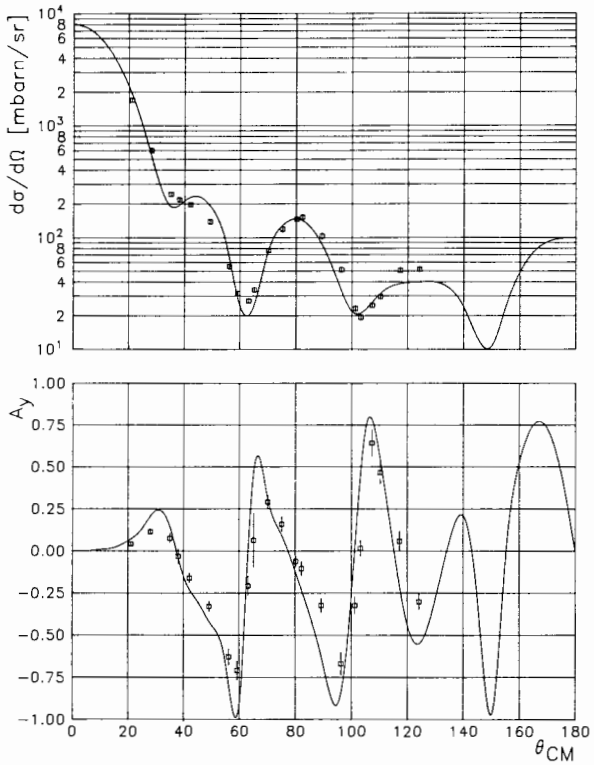

Fig. 10: Differential cross section and analysing power of ^{nat}Pb together with microscopic optical model results.

Both isotopes of ^{nat}**Cu** can be described in terms of the excited core model, too. Here a $2p_{3/2}$ proton couples to a harmonic vibrational Ni – core [7,8] . The geometrical parameters of ^{63}Cu and ^{65}Cu are equal, whereas the deformations are different. The quartet arising from the first excited 2^+ – Ni-core could be observed, although unresolved. According to the above model nuclear reduced matrix elements could be specified, thus allowing a successful parameter search for the mixture of both isotopes (see Fig. 8).

Microscopic Potentials

Differential cross section and analysing power data for ^{89}**Y** and ^{nat}**Pb** have been analysed with a renormalized microscopic potential of the Brieva-Rook-von Geramb type [9], which was provided in tabulated form [10]. Emphasizing the fact that these potentials were applied without any change of geometry, they lead to quite promising model fits. See Figs. 9 and 10 for the results. The analysis with a similar approach of Yamaguchi et.al. [11] and with the effective potentials of Jeukenne et.al. [12] is in progress.

REFERENCES

[1] J.W. Hammer, G. Bulski, W. Grum, W. Kratschmer, H. Postner, and G. Schleußner, NIM **244**, 455 (1986).

[2] E. Woye, code JANE, private communication. W. Grum, code XJANE, unpublished.

[3] J. Raynal, coupled-channels code ECIS79, 1979 (NEA Data Bank).

[4] G.M. Honoré, W. Tornow, C.R. Howell, R.S. Pedroni, R.C. Byrd, R.L. Walter, and J.P. Delaroche, Phys.Rev. C**33**, 1129 (1986).

[5] C.S. Whisnant, J.H. Dave, and C.R. Gould, Phys.Rev. C**30**, 1435 (1984).

[6] F. Fabbri, G. Fratamico, and G. Reffo, Hauser-Feshbach code CERBERO3, NEA Data Bank (1977).

[7] S.M. El-Kadi, C.E. Nelson, F.O. Purser, R.L. Walter, A. Beyerle, C.R. Gould, and L.W. Seagondollar, Nucl.Phys. **A390**, 509 (1982).

[8] J.P. Delaroche, S.M. El-Kadi, P.P. Guss, C.E. Floyd, and R.L. Walter, Nucl.Phys. **A390**, 541 (1982).

[9] H.V. von Geramb, F.A. Brieva, and J.R. Rook, in *Microscopic optical potentials*, Hamburg 1978, ed. H.V. von Geramb, Springer, Berlin, 1979.

[10] H.V. von Geramb, private communication, May 1985.

[11] N. Yamaguchi, S. Nagata, and T. Matsuda, Prog.Theor.Phys. **70**, 459 (1983).

[12] J.-P. Jeukenne, A. Lejeune, and C. Mahaux, Phys.Rev. C**16**, 80 (1977). A. Lejeune, Phys.Rev. C**21**, 1107 (1980).